Practical method for full curved-wave theory analysis of experimental extended x-ray-absorption fine structure

A. G. McKale,* G. S. Knapp, and S.-K. Chan
Materials Science and Technology Division, Argonne National Laboratory, Argonne, Illinois 60439
(Received 2 August 1985)

Recent work has indicated that the single-scattering theory of x-ray absorption may be valid down to much closer to the edge than previously thought. It is in this region that the plane-wave approximation used in the standard extended x-ray-absorption fine structure analysis breaks down. Using a simple reformulation, we obtain modified backscattering amplitude and phase-shift functions which are similar to those of Teo and Lee but which use the full curved-wave theory for single scattering. These can then be used to analyze experimental data without any modification of those programs that presently use the functions of Teo and Lee. We also present results of using this method to compare experimental data with theoretical calculations for copper metal and NiO.

X-ray absorption spectroscopy is a useful probe of the local structure of materials. Traditionally, spectra have been divided into two regions: the x-ray-absorption near-edge structure (XANES) region, which lies up to ≈ 40 eV above the edge, and the extended x-ray-absorption fine-structure (EXAFS) region, which lies beyond ≈ 40 eV above the edge.[1-5] This division has been based on the belief that a number of factors that are relatively insignificant in the EXAFS region become important close to the edge such as multiple scattering, chemical effects, and the curvature of the outgoing photoelectron wave function.

It was assumed that while a single scattering formalism is valid in the EXAFS region, multiple scattering must be taken into account in the XANES region. This assumption has recently been called into question by Müller and Schaich[6] and by Bunker and Stern.[7] Their work indicates that a single scattering theory can generally be applied, not only in the EXAFS region, but well down into the XANES region (at least down to 15 eV above the edge). One might expect that close to the edge the spectra would be highly sensitive to chemical bonding and, indeed, there is extensive literature showing correlation between edge shifts and valence states. It has been shown,[8,9] however, that above the edge these chemical effects are correlated with structural changes, i.e., changes in near-neighbor distances. Other effects of chemical bonding are only significant very close to or below the edge. The appearance of sensitivity to chemical bonding above the edge is really sensitivity to structure. The breakdown of the plane-wave approximation at low photoelectron energies amplifies the effect of structural differences on the spectra. If the photoelectron wave function is not approximated by a plane wave, but rather the full curved-wave formalism is used, it is seen that most of the observed chemical effects are associated with structural changes.

If comparison of experimental data and theoretical calculations is to be made at low energies it is necessary to use the full curved wave formalism. We present a very straightforward way to do this without modification of existing EXAFS plane-wave–type codes that use the *ab initio* calculations of the backscattering amplitude and phase-shift functions of Teo and Lee.[4]

This improvement provides a simple access to data much closer to the edge than was previously used thereby increasing the utility of EXAFS. Such data are of the utmost importance for the study of disordered systems and materials that contain backscattering atoms of low atomic number, because the EXAFS spectra in these situations decays rapidly with increasing energy and much of the information lies in the XANES region.

In the EXAFS region the standard procedure has been to focus on the modulation of the absorption coefficient $\chi_l(k)$ using the standard EXAFS equation:[1-3,5,10-12]

$$\chi_l(k)=\mathrm{Im}\left[\sum_j (-1)^l \frac{F_j(k)N_j\gamma_j}{kR_j^2} \times \exp\{i[2kR_j+2\delta_c+\Phi_j(k)]\}e^{-2k^2\sigma_j^2}\right], \tag{1}$$

where l is the angular momentum of the final state, F_j is the backscattering amplitude from each of the N_j neighboring atoms in the jth shell which are located at an average distance R_j from the absorbing atom. To account for the effect of inelastic processes an empirical, k-independent scaling factor, γ_j, is used. These processes include the inelastic scattering of the photoelectron by the neighboring atom and the medium in between,[13] inelastic losses at the absorbing atom, and the lifetime of the core hole[14] and hence should have a k dependence.[13,15] The second exponential containing σ_j^2 is a Debye-Waller–type term where σ_j is the MSRD (mean-square radial displacement) of the atoms about R_j. The parameter δ_c is the phase shift due to the central atom and $\Phi_j(k)$ is the phase shift due to the backscattering atom. The backscattering amplitude and phase shift are related to the individual partial-wave phase shifts of the neighboring atoms by

$$F_j e^{i\Phi_j}=\frac{1}{k}\sum_{l'}(2l'+1)(-1)^{l'}e^{i\delta_{l'}}\sin\delta_{l'} . \tag{2}$$

Implicit in Eq. (1) is the plane-wave approximation

which is valid when the energy of the photoelectron is sufficiently high so that the outgoing wave function can be accurately approximated by a plane wave. Below this energy, generally taken to be 40 eV above the edge, this approximation breaks down and Eq. (1) does not hold.

Using the full curved-wave formalism, following the notation of Schaich,[16] we have

$$\chi_l = \mathrm{Im} \sum_j \left[N_j \gamma_j e^{i\delta_c} \sum_{l'} \{ (2l'+1) e^{i\delta_{l'}} \sin\delta_{l'} \times [H(l,l';R_j)] e^{-2k^2\sigma_j^2} \} \right], \quad (3)$$

where

$$H(l,l';R_j) = \sum_{\bar{l}} (2\bar{l}+1) \left\{ \begin{bmatrix} l & l' & \bar{l} \\ 0 & 0 & 0 \end{bmatrix} [h_{\bar{l}}^{+}(kR_j)] \right\}^2 \quad (4)$$

with the first factor in the curly brackets in Eq. (4) being a $3j$ symbol and $h_{\bar{l}}^{+}(kR_j)$ being an outgoing spherical Bessel function.[17] Various sum rules can be used to simplify Eq. (4) given knowledge of the symmetry of the scattering wave.

For K-shell absorption, the final state must have p symmetry, i.e., $l=1$, and Eq. (4) becomes

$$H(1,l';R_j) = \frac{l'+1}{2l'+1} [h_{l'+1}^{+}(kR_j)]^2 + \frac{l'}{2l'+1} [h_{l'-1}^{+}(kR_j)]^2 .$$

For L-shell absorption, the final state can have either s or d symmetry. However, it has been shown that the contribution to $\chi(k)$ from the s part is negligible compared to that from the d part.[4,18] Using only the $l=2$ part,

$$H(2,l';R_j) = \frac{3l'(l'-1)}{2(2l'+1)(2l'-1)} [h_{l'-2}^{+}(kR_j)]^2 + \frac{l'(l'+1)}{(2l'+3)(2l'-1)} [h_{l'}^{+}(kR_j)]^2 + \frac{3(l'+2)(l'+1)}{2(2l'+3)(2l'+1)} [h_{l'+2}^{+}(kR_j)]^2 .$$

The expressions H in Eq. (4), although cumbersome are not computationally difficult. However, they involve mixing of structural information, R_j, with the electronic

TABLE I. Backscattering amplitudes $f(k)$ in Å versus photoelectron wave vector k in Å^{-1}. [Note that the scale used for the photoelectron wave vector above 3.5 Å^{-1} is the same as that of Teo and Lee (Ref. 4).]

		k					
		1.865 76	2.344 29	2.822 58	3.300 96	3.779 39	4.257 77
		4.724 18	5.196 53	5.669 03	6.141 44	6.661 24	7.086 31
		7.558 68	8.503 57	9.448 37	10.393 23	11.338 10	12.282 88
Element	Radius	13.227 76	14.172 53	15.117 41			
O	2.10	1.101 73	0.992 67	0.883 72	0.775 77	0.670 86	0.573 70
		0.491 03	0.420 53	0.361 83	0.310 99	0.260 15	0.222 22
		0.190 66	0.157 59	0.123 23	0.096 12	0.079 23	0.063 47
		0.051 15	0.048 44	0.043 24			
O	3.75	1.159 15	1.050 08	0.939 90	0.820 00	0.707 24	0.608 91
		0.523 56	0.446 85	0.381 24	0.325 32	0.272 01	0.233 48
		0.211 85	0.149 72	0.114 47	0.098 96	0.078 55	0.059 29
		0.057 94	0.039 84	0.043 08			
Ni	2.75	0.172 07	0.294 66	0.365 19	0.262 27	0.283 02	0.449 07
		0.541 07	0.601 86	0.729 41	0.775 51	0.779 30	0.787 06
		0.787 02	0.707 34	0.617 38	0.529 18	0.439 07	0.374 08
		0.310 83	0.293 43	0.240 78			
Ni	4.00	0.584 04	0.515 72	0.465 40	0.375 31	0.335 61	0.437 88
		0.517 01	0.593 01	0.708 34	0.768 92	0.779 58	0.792 05
		0.795 35	0.721 73	0.632 03	0.542 51	0.450 45	0.384 55
		0.318 79	0.222 26	0.125 24			
Cu	2.75	0.501 81	0.422 21	0.347 43	0.283 25	0.266 05	0.323 49
		0.423 44	0.527 36	0.617 79	0.686 82	0.733 71	0.751 86
		0.754 57	0.714 35	0.637 03	0.551 84	0.468 68	0.396 45
		0.334 48	0.272 48	0.264 09			
Cu	4.00	0.613 33	0.568 74	0.483 67	0.389 36	0.325 66	0.335 26
		0.408 45	0.506 38	0.598 22	0.672 64	0.727 16	0.749 78
		0.758 77	0.725 05	0.650 35	0.565 74	0.480 34	0.406 07
		0.343 03	0.315 38	0.288 25			

properties of the backscattering atoms embodied in δ_l in a complicated way. The crucial step is to recognize that we can recast Eq. (3) to the plane-wave form [Eq. (1)]:

$$\chi_l(k)=\mathrm{Im}\left[\sum_j (-1)^l \frac{f_j(k,kR)N_j\gamma_j}{kR_j^2} \times\exp\{i[2kR_j+2\delta_c+\phi_j(k,kR)]\}e^{-2k^2\sigma_j^2}\right],$$

where the backscattering amplitude, f_j, and phase shift, ϕ_j, are now functions of k and R_j. Given the partial phase shifts, δ_l, and an R_j, the exact $\chi(k)$ is easily calculated (even on a microcomputer) and the functions $f_j(k,kR)$ and $\phi_j(k,kR)$ extracted. These functions are weak functions of R. Hence, functions calculated at a given R_j can be used for a range about that value without significantly altering the structural parameters obtained from the analysis. We tested this by fitting our data with backscattering amplitudes and phase shifts generated using various values for R_j. No significant variation in the final structural parameters was found over a range of R values. The difference between the functions at different values of R_j is compensated for by a slight variation in E_0 (± 0.8 eV), the initial electron binding energy. Thus by calculating the backscattering amplitude and phase-shift functions at a few select values of R_j, we can use the full curved-wave formalism within existing codes.

To illustrate the power of the technique we need to compare both the plane-wave and curved-wave theory with experiment. Measurements were made on copper metal and nickel oxide using the Argonne focusing crystal EXAFS facility.[19] The measurements on copper were made at a resolution of 6 eV, those on NiO at 3 eV. Deconvolution procedures were used on the copper data to remove the effects of low resolution. The copper sample was a thin high purity foil with no apparent pinholes. The NiO sample was four layers of $>99.99\%$ purity powder brushed uniformly onto Scotch tape. Both samples had absorption coefficients of less than 2. By running the x-ray generator at a sufficiently low voltage higher-order harmonic contamination was avoided. The $k\chi(k)$ for Cu at 80 K was compared to spectra reported by several authors and found to be nearly identical.

To obtain the partial-wave phase shifts, δ_l, the radial

TABLE II. Backscattering phase shifts $\phi(k)$ in radians versus photoelectron wave vector k in Å^{-1}. [Note that the scale used for the photoelectron wave vector above 3.5 Å^{-1} is the same as that of Teo and Lee (Ref. 4).]

		k					
		1.865 76	2.344 29	2.822 58	3.300 96	3.779 39	4.257 77
		4.724 18	5.196 53	5.669 03	6.141 44	6.661 24	7.086 31
		7.558 68	8.503 57	9.448 37	10.393 23	11.338 10	12.282 88
Element	Radius	13.227 76	14.172 53	15.117 41			
O	2.10	0.814 94	0.438 07	0.088 34	−0.189 23	−0.393 83	−0.552 92
		−0.670 95	−0.762 24	−0.856 45	−0.962 00	−1.070 87	−1.139 24
		−1.199 80	−1.430 42	−1.629 97	−1.714 58	−1.894 73	−2.171 33
		−2.178 72	−2.389 19	−2.605 34			
O	3.75	0.254 47	−0.000 81	−0.234 95	−0.425 72	−0.593 76	−0.713 34
		−0.798 23	−0.870 77	−0.959 43	−1.045 90	−1.129 02	−1.180 27
		−1.232 81	−1.521 57	−1.665 67	−1.849 93	−2.018 55	−2.018 15
		−2.252 14	−2.386 01	−2.404 96			
Ni	2.75	4.509 12	4.749 39	4.461 52	4.237 12	4.868 75	5.081 05
		5.069 25	5.104 57	5.075 59	4.981 21	4.912 23	4.883 55
		4.849 49	4.733 03	4.607 60	4.467 54	4.300 88	4.144 54
		3.963 99	3.778 90	3.657 70			
Ni	4.00	4.202 76	4.155 89	4.017 16	3.856 15	4.241 43	4.648 88
		4.762 51	4.833 16	4.860 84	4.786 38	4.765 35	4.742 87
		4.717 70	4.640 12	4.528 19	4.410 18	4.250 48	4.105 31
		3.900 63	3.815 14	3.745 33			
Cu	2.75	3.773 66	3.714 63	3.678 48	3.770 82	4.121 56	4.444 28
		4.600 18	4.658 83	4.676 61	4.674 03	4.657 64	4.636 82
		3.606 36	4.542 29	4.455 41	4.342 19	4.220 12	4.075 45
		3.929 62	3.809 16	3.664 75			
Cu	4.00	3.604 37	3.460 28	3.330 80	3.354 34	3.591 49	3.960 47
		4.246 12	4.378 30	4.450 85	4.482 24	4.490 66	4.484 20
		4.482 70	4.448 62	4.368 74	4.281 04	4.156 95	4.028 37
		3.876 57	3.759 24	3.648 09			

Schrödinger equation for an outgoing electron was solved at energy $E=\hbar^2/2mk^2$ in the Hartree-Fock approximation. Herman-Skillman wave functions were used for the core electrons. The outer electrons were assumed to be smeared uniformly and an appropriate charge density was used as compensation to achieve a constant potential equal to $V(r)$ at $r=R$ outside the muffin-tin radius, R which is chosen to be approximately equal to the ionic or covalent radius of the ion. The radial Schrödinger equation was then integrated outwards from the origin and matched at R to the outgoing free-space solution to obtain δ_l. No inelastic scattering processes are included in this calculation.

The partial-wave phase shifts were then used to generate the plane-wave and curved-wave backscattering amplitude and phase-shift functions for each element. We chose to evaluate the curved-wave functions at $R_j=2.75$ and 4.00 Å for metallic elements and at $R_j=2.1$ and 3.5 Å for oxygen. These distances were chosen because, while we know the actual values of the interatomic distances in the cases under investigation, we wanted to choose distances that were generally close to the values encountered over a range of systems, e.g., the average first-shell distance for metallic systems is about 2.75 Å. The backscattering amplitude and phase-shift functions for O, Cu, and Ni are tabulated in Tables I and II. They are usable in exactly the same way as the tabulations of Teo and Lee.[4]

After background removal, the data was Fourier filtered to isolate the contribution from a selected region in real space, and curve fitting procedures were used to determine the structural parameters.[20] In the fitting routine E_0, R_j, and $N_j\gamma_j$ were allowed to vary in the neighborhood of reasonable initial values until a best fit was obtained. When using the backscattering amplitude and phase-shift functions obtained from the plane-wave approximation, only those data with $k>4$ Å^{-1} were used for the actual fitting. When the full curved-wave formalism was used, all the information for $k>1.8$ Å^{-1} was included. The Debye-Waller–type factors were obtained from theory[21] in the case of Cu, and were determined experimentally by using the ratio method[2,22] in conjunction with measurements at 77 and 298 K in the case of NiO. The central atom phase shifts, as determined by Teo and Lee,[4] were used.

We used the backscattering amplitude and phase-shift functions as calculated at 2.75 Å for the first shell of copper and at 4.00 Å for the other three shells. For NiO, we used the functions calculated at 2.10 Å for the first oxygen shell and 2.75 Å for the first nickel shell. The experimental spectra and the theoretical fits are shown in Figs. 1 and 2. In each case a noticeable improvement for $k<4$

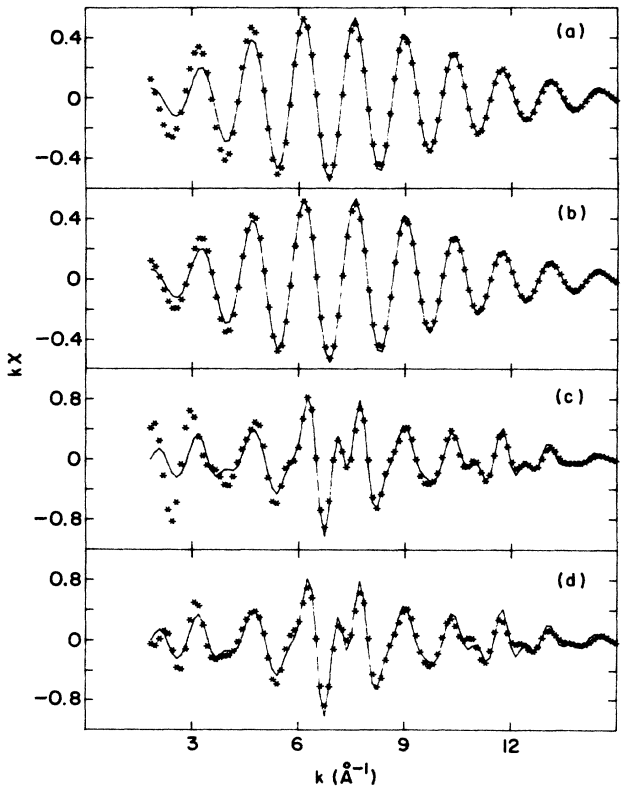

FIG. 1. Experimental (solid line) and theoretical (asterisks) EXAFS spectra for copper metal at 77 K. (a) and (b) are for the first shell only; (c) and (d) are for the first four shells. (a) and (c) use the plane-wave approximation in the calculation of the theory; (b) and (d) use the full curved-wave formalism.

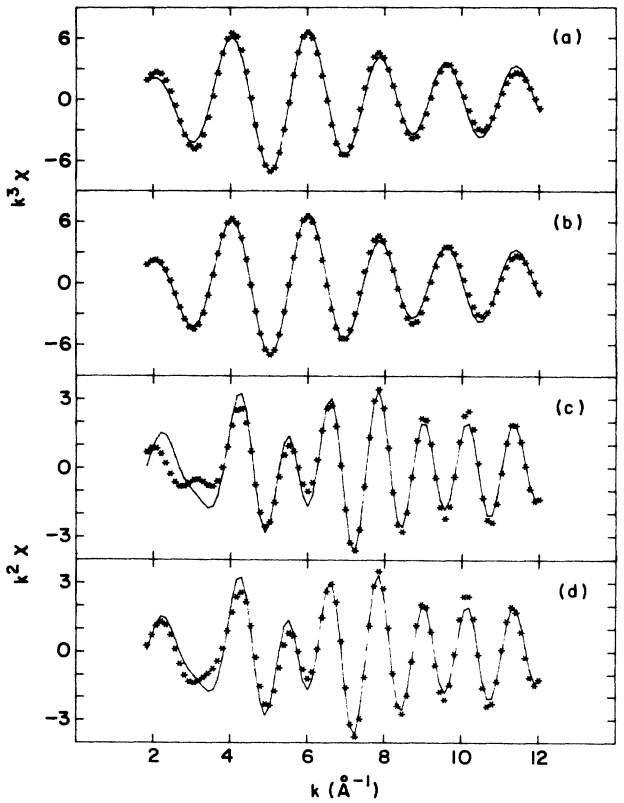

FIG. 2. Experimental (solid line) and theoretical (asterisks) EXAFS spectra for NiO at 77 K. (a) and (b) are for the first shell only; (c) and (d) are for the first and second shells. (a) and (c) use the plane-wave approximation in the calculation of the theory; (b) and (d) use the full curved-wave formalism.

TABLE III. Radial distances in Å derived from EXAFS spectra and known crystallographic values.

	Plane wave	Curved wave	Known crystallographic value
Cu			
R_1	2.54±0.01	2.54±0.01	2.556
R_2	3.56±0.02	3.59±0.02	3.615
R_3	4.40±0.01	4.45±0.01	4.427
R_4	5.06±0.01	5.11±0.01	5.112
NiO			
R_1	2.05±0.01	2.08±0.01	2.084
R_2	2.93±0.01	2.96±0.01	2.948

$Å^{-1}$ is obtained with the use of the full curved-wave formalism, both in the phase and the amplitude. For $k > 4$ $Å^{-1}$ the plane-wave approximation is reasonably valid so there is little difference between the agreements.[23]

We have also fit the data using the backscattering amplitude and phase-shift functions, f and ϕ, calculated at the known crystallographic values. No significant difference in the deduced parameters, i.e., E_0, R_j, and $N_j\gamma_j$, was encountered as a result of using the approximate R_j values in the calculation of the backscattering amplitude and phase shift.

The radial distances obtained using the plane-wave approximation and the curved-wave formalism are tabulated in Table III along with the known crystallographic values. The curved-wave approach results in a better determination of all interatomic distances. While the plane-wave approximation should be adequate for higher shells, it must be remembered that we are fitting all the shells at one time. The use of inappropriate, i.e., plane-wave, parameters for the first shell results in slight errors in the distance determination for higher shells because there is some overlap in the Fourier components from each shell. It is possible to use curved-wave parameters for the first shell and plane-wave parameters for higher shells, but there is little reason to do so.

The improvement in distance determination is much more striking in the case of NiO. This is attributable to the smaller range of data and the smaller number of oscillations present in the data. In the case of Cu the data extends over a larger range because there are more nearest neighbors and because the nearest neighbors have stronger backscattering potentials. Furthermore, the first near-neighbor distance is greater in Cu so there are more oscillations. Both of these factors reduce the significance of the data below 4 $Å^{-1}$ to parameter determination. The use of the curved-wave formalism is even more important for most materials whose structure we might want to determine. Such materials are often more disordered than either Cu or NiO, hence good data can be obtained only over a more limited range.

We also obtain the product $N_j\gamma_j$. The extraction of the number of atoms, N_j, requires knowledge of the scaling factor, γ_j, which accounts for inelastic processes. Generally this knowledge is obtained from known chemical systems that are presumed to be similar to the system under investigation. In the case of *ab initio* calculations we do not have this information. If the number of atoms is known, information about the scaling factor can be obtained. Even without inclusion of any inelastic processes in our calculation of the theoretical backscattering functions we get a scaling factor that is comparable to that obtained through the use of the functions of Teo and Lee.

We have also generated the backscattering amplitude and phase-shift functions for a number of other elements including Pb, Pt, Th, U, Pu, and Np. In the case of L-shell absorption we find the k dependence of the inelastic processes to be more pronounced as is to be expected given the shorter core hole lifetimes of these elements. However, these effects are amplitude effects and do not interfere with the ability to determine bond lengths. For example, for Pt, NpAs, ThAs, and PuAs the EXAFS determined first-shell distance agrees to within 0.01 Å of the known distance. To determine coordination number better methods of dealing with these inelastic effects are needed.

We have presented a straightforward method whereby experimentalists can use *ab initio* calculations of the backscattering amplitude and phase shift with the full curved-wave formalism of EXAFS theory without any more effort than is now needed to use plane-wave theory. This allows easy access to data much closer to the edge than was previously used and should increase the ability to study disordered systems and materials that contain backscattering atoms of low atomic number and the utility of EXAFS in general. All that is required is the generation and publication of tables similar to those of Teo and Lee, a task we are presently engaged in.

Note added in proof. We would like to thank John Rehr for bringing to our attention a somewhat similar approach that he and his colleagues have developed (unpublished).

We are grateful to B. Veal, D. Lam, P. Montana, and G. Shenoy for their helpful discussions and careful reading of this manuscript. This work was supported by the U. S. Department of Energy (Office of Basic Energy Sciences, Division of Materials Science) under Contract No. W-31-109-Eng-38.

*Also at Department of Physics, Northwestern University, Evanston, IL 60201.

[1]D. E. Sayers, E. A. Stern, and F. W. Lytle, Phys. Rev. Lett. **27**, 1204 (1971).

[2]E. A. Stern, D. E. Sayers, and F. W. Lytle, Phys. Rev. B **11**, 4836 (1975).

[3]P. A. Lee and J. B. Pendry, Phys. Rev. B **11**, 2795 (1975).

[4]B. K. Teo and P. A. Lee, J. Am. Chem. Soc. **101**, 2815 (1979).

[5]E. A. Stern, Phys. Rev. B **10**, 3027 (1974).

[6]J. E. Müller and W. L. Schaich, Phys. Rev. B **27**, 6489 (1983).

[7]G. B. Bunker and E. A. Stern, Phys. Rev. Lett. **52**, 1990 (1984).

[8]B. A. Bunker and E. A. Stern, Phys. Rev. B **27**, 1017 (1983).

[9]G. B. Bunker, Ph.D. dissertation, University of Washington (1984).

[10]W. L. Schaich, Phys. Rev. B **8**, 4028 (1973).

[11]C. A. Ashley and S. Doniach, Phys. Rev. B **11**, 1279 (1975).

[12]J. J. Boland, S. E. Crane, and J. D. Baldeschwieler, J. Chem. Phys. **77**, 142 (1982).

[13]E. A. Stern, B. A. Bunker, and S. M. Heald, Phys. Rev. B **21**, 5521 (1980).

[14]W. Ekardt and D. B. T. Doi, Solid State Commun. **40**, 939 (1981).

[15]E. A. Stern, S. M. Heald, and B. A. Bunker, Phys. Rev. Lett. **42**, 1372 (1979).

[16]W. L. Schaich, Phys. Rev. B **29**, 6513 (1984). See also S. J. Gurman, N. Binsted, and I. Ross, J. Phys. C **17**, 143 (1984); and J. J. Barton and D. A. Shirley, Phys. Rev. B **32**, 1862 (1985).

[17]See, for instance, A. Messiah, *Quantum Mechanics* (North-Holland, Amsterdam, 1966).

[18]S. M. Heald and E. A. Stern, Phys. Rev. B **16**, 5549 (1977).

[19]G. S. Knapp and P. Georgopoulos, in *Laboratory EXAFS—1980 (Univeristy of Washington)*, proceedings of the Workshop on Laboratory EXAFS Facilities and Their Relation to a Synchrotron Radiation Source, edited by E. A. Stern (AIP, New York, 1980).

[20]C. Tang *et al.*, Phys. Rev. B **31**, 1000 (1985).

[21]E. Sevillano, H. Meuth, and J. J. Rehr, Phys. Rev. B **20**, 4908 (1979).

[22]G. B. Bunker, Nucl. Instrum. Methods **207**, 437 (1983).

[23]There is a slight degradation of the agreement at high k in the case of the first four shells of copper using the curved wave formalism [Fig. 1(d)]. This is the result of the larger range over which the data is fit. The plane-wave parameters are fit only for $k > 4$ Å^{-1} because we know that the plane-wave approximation is not valid below 4 Å^{-1}. Hence the region above 4 Å^{-1} is more heavily weighted in this case than in the case of the fit using the curved wave formalism where the whole range is used. If the plane-wave parameters are used over the entire range the agreement at all k values is greatly reduced. If the curved wave parameters are used to fit only the data with $k > 4$ Å^{-1} we obtain a fit that is as good as that obtained using the plane-wave approximation [Fig. 1(c)] in the region above 4 Å^{-1} but the agreement at low k is not as good as that obtained using the curved wave parameters over the entire range [Fig. 1(d)].